

Niobium: Lattice Parameter and Density

Cite as: Journal of Applied Physics **39**, 4044 (1968); <https://doi.org/10.1063/1.1656912>

Submitted: 21 January 1968 . Published Online: 19 November 2003

R. L. Barns



View Online



Export Citation

ARTICLES YOU MAY BE INTERESTED IN

[Superconducting properties and crystal structures of single-crystal niobium nitride thin films deposited at ambient substrate temperature](#)

Journal of Applied Physics **79**, 7837 (1996); <https://doi.org/10.1063/1.362392>

[Structural characterization of niobium oxide thin films grown on SrTiO₃ \(111\) and \(La,Sr\)\(Al,Ta\)O₃ \(111\) substrates](#)

Journal of Applied Physics **120**, 245302 (2016); <https://doi.org/10.1063/1.4972830>

[Elastic Constants of Niobium from 4.2° to 300°K](#)

Journal of Applied Physics **36**, 3689 (1965); <https://doi.org/10.1063/1.1703072>

HIDEN
ANALYTICAL

Instruments for Advanced Science

- Knowledge,
- Experience,
- Expertise

[Click to view our product catalogue](#)

Contact Hiden Analytical for further details:

www.HidenAnalytical.com
info@hiden.co.uk

Gas Analysis

- ▶ dynamic measurement of reaction gas streams
- ▶ catalyst and thermal analysis
- ▶ molecular beam studies
- ▶ dissolved species probes
- ▶ fermentation, environmental and ecological studies

Surface Science

- ▶ UHV-TPD
- ▶ SIMS
- ▶ end point detection in ion beam etch
- ▶ elemental imaging - surface mapping

Plasma Diagnostics

- ▶ plasma source characterization
- ▶ etch and deposition process reaction kinetic studies
- ▶ analysis of neutral and radical species

Vacuum Analysis

- ▶ partial pressure measurement and control of process gases
- ▶ reactive sputter process control
- ▶ vacuum diagnostics
- ▶ vacuum coating process monitoring

AIP
Publishing

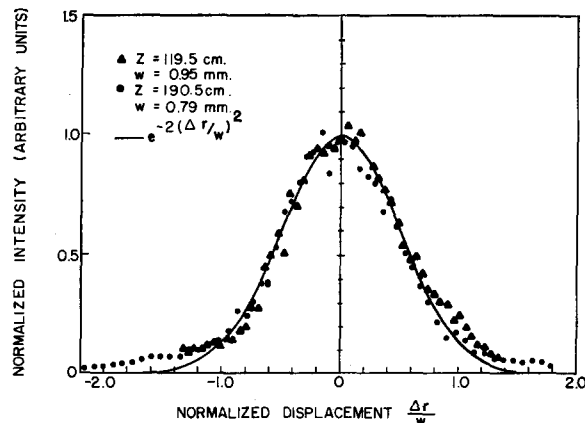


FIG. 1. Normalized beam intensity as a function of the normalized displacement $\Delta r/w_0$ from beam center. Results for two distances z from the laser output mirror are shown. The spatial resolution was determined by an 18μ pinhole.

Single-mode operation was also obtained using spherical mirrors in cavities between confocal and concentric as has been previously reported,² but we found that proper adjustment of such a curved mirror system was far more difficult. In addition, the TEM₀₀ modes were less Gaussian for these cavities and the output powers were lower because of the smaller mode volumes. On the other hand, it was possible to achieve single-mode operation over more regions of the rod than with flat mirrors.

We have been using the single-mode laser for over a year and our experience with the dielectric mirrors has been good as long as the laser is mode controlled. They have been used without degradation at power densities of 100 MW/cm². Without mode control, however, the mirrors are rapidly destroyed at average power densities far less than this amount. This could be due to the "hot spots" that appear in non-mode-controlled lasers or to the spontaneous appearance of psec pulses.³

The Q-switch cells we have used are not AR-coated and are placed in the cavity at an angle of several degrees. When a 1 cm path length cell is used, stimulated Brillouin scattering occurs in the methanol and the output pulse is distorted in time as well as being multifrequency.⁴ With a cell having a 2 mm path length, this problem has not been encountered.

The in-cavity power depends only very slightly upon the output mirror transmission as long as it is less than about 75%. Thus, maximum power output is usually obtained using a sapphire resonant reflector. The longitudinal-mode-selecting properties of the laser are not dependent upon the use of such reflectors, however, and dielectric-coated wedged output mirrors give just as pure a mode spectrum. The longitudinal mode selection appears to be due to the properties of the bleachable dye Q-switch.^{2,5}

The best monitor of the purity of the longitudinal-mode spectrum is observation of the time dependence of the output pulse. A Tektronix 519 oscilloscope in conjunction with a TRG 105B photodiode is used for this purpose. The time trace of a single-mode shot is a smooth curve resembling a Gaussian. If two modes are present (we have never seen more than two), the beat between the modes is clearly visible as a sinusoidal modulation of the normal single-mode output pulse at a frequency $nc/2L$, where n is an integer (usually 4 for our laser) and $c/2L$ is the frequency spacing between adjacent axial modes.⁶ Observation of the time trace is a more sensitive indicator of mode purity than is a photograph of the Fabry-Perot spectrum. Often the presence of a weak second mode is not indicated by observing the Fabry-Perot ring system whereas it is unmistakably shown by a small degree of "ripple" on the time trace. In addition, occasionally the laser will double pulse, the two pulses being single-mode but

at different frequencies. The resulting Fabry-Perot photograph shows two ring systems and is ambiguous.

The nature of the transverse mode has been investigated in several ways, all of them showing that it is very nearly Gaussian. The results shown in Fig. 1 were obtained by scanning the beam with a photodiode mounted behind an 18μ pinhole (the pinhole was made in 0.003 in. phosphor bronze using the laser and a 17 mm lens). Since each point in the diagram represents a separate firing of the laser, the over-all scan attests to the repeatability of the spatial mode of the laser. For these measurements the photodiode was in the near-to-intermediate field of the laser. Notice that the output beam was slightly convergent; for other setups (a different rod or a different spot in the same rod), a diverging output was obtained. Assuming Gaussian beam propagation and fitting the parameters to a set of measurements like those shown in Fig. 1 yields a half-angle beam divergence $\delta \approx 2.6 \times 10^{-4}$ rad. The fact that the wavefronts are not planar on the mirrors most probably is due to focusing effects in the ruby or in the bleachable liquid.

An alternative determination of the temporal and spatial coherence of the output beam was reported elsewhere⁷ by showing that the laser could be used as a source for making diffraction-limited holograms.

In summary, we have reported on a simple means for obtaining single-longitudinal- and transverse-mode operation from a passively Q-switched ruby laser. The output beam from such a laser can be effectively used in experiments in areas such as nonlinear optics or holography where the coherence properties of the radiation are important.

¹ Hans W. Mocker and R. J. Collins, *Appl. Phys. Letters* **7**, 270 (1965).

² V. Daneu, C. A. Sacchi, and O. Svelto, *IEEE J. Quantum Electron.* **QE-2**, 290 (1966).

³ M. A. Duguay, S. L. Shapiro, and P. M. Rentzepis, *Phys. Rev. Letters* **19**, 1014 (1967).

⁴ A. J. Alcock and C. DeMichelis, *Appl. Phys. Letters* **11**, 42 (1967).

⁵ W. R. Sooy, *Appl. Phys. Letters* **7**, 36 (1965).

⁶ M. Hercher, *Appl. Phys. Letters* **7**, 39 (1965).

⁷ J. T. LaMacchia and J. E. Bjorkholm, *Appl. Phys. Letters* **12**, 45 (1968).

Niobium: Lattice Parameter and Density

R. L. BARNES

Bell Telephone Laboratories, Incorporated, Murray Hill, New Jersey

(Received 21 January 1968)

In order to check the agreement to be expected between the densities of a material as calculated from hydrostatic measurements and x-ray measurements (henceforth referred to as hydrostatic density and x-ray density), the density of a single crystal of niobium was measured by both techniques. Niobium was chosen because it is available in reasonably large single crystals of relatively high purity, it is monoisotopic, and it has a rather high density (which should make the hydrostatic measurement less accurate).

TABLE I. Hydrostatic density data.

Temp. (°C)	23.5	23.8
Density of CCl ₄ ^a	1.58726	1.58667
Calc. density (corrected for air buoyancy)	8.57644	8.57498
Thermal expansion coefficient	7.1 ppm/°C ^b	
Calc. density corrected to 25°C	8.57605	8.57467
Avg. 8.5754 g/cc ± 0.0010		

^a *International Critical Tables*, (McGraw-Hill Book Co., New York), Vol. 3.

^b *American Institute of Physics Handbook*, 2nd ed. (McGraw-Hill Book Company, New York, 1963).

TABLE II. X-ray density data.

$\lambda \text{ CuK}\alpha_1 = 1.540562 \text{ \AA}$ 25.0°C (330) reflection.	
Uncorrected θ 82°0' 26.4" \pm 1.3" (avg. of 4 meas.)	
a (corrected for refraction, axial divergence, and Lorentz-polarization errors)	3.300208 $\text{\AA} \pm 0.000002$
Average linewidth	15'33" \pm 6"
Spectral+slit width	7'11"
Crystal linewidth	8'22" \pm 6"
Avogadro's number	6.022135 ^a $\pm 0.00015 \times 10^{23}$
Atomic weight	92.90602 ^b
Density (x-ray)	8.58368 ± 0.00021 g/cc

^a J. A. Bearden, U.S.A.E.C., Oak Ridge, Tenn. (1964), p. 520.

^b L. A. Konig, Nucl. Phys. 31, 28 (1962).

The sample was grown from Ciba material which the manufacturer reported as containing 300–500 atomic ppm carbon and oxygen and 0–100 atomic ppm tantalum. The crystal was grown by a vacuum electron-beam floating-zone method. The resistance ratio $R_{300^\circ}/R_{4.2^\circ} = 950 \pm 150$ (W. A. Reed, private communication).

The hydrostatic density was measured by weighing a 7 g section in CCl_4 and in air. Corrections were made as in Ref. 1. The results are shown in Table I. The standard deviation of the density was estimated from a series of ten replicates on two samples of silica glass. All error estimates (σ) given are standard deviations.

The lattice parameter was measured by Bond's method^{2,3} on a heavily etched spark-cut surface. The diffraction linewidth was measured at three locations on a 3 mm² surface. The full widths at half-max. (at a theta of 82°) due to the crystal (after subtracting the spectral and slit width) were 20, 12, and 8.3 arc min. The location with 8.3' was used for measuring the lattice parameter. The results are shown in Table II. All of the uncertainty in the x-ray density is due to the uncertainty in Avogadro's number.

The two densities disagree by 1 part in 1000 (which is more than 3σ), with the hydrostatic density being smaller than the x-ray density. Taking the extreme values of the hydrostatic density ($+3\sigma$ and -3σ) gives the range for the fractional concentration of vacancies as 1.3×10^{-3} to 7×10^{-4} . Since

$$n/N = A \exp(-E_f/kT) = 0.014,$$

where n =No. of vacancies, N =No. of atoms $A=1$, $E_f=1 \text{ eV}$,⁴ and $T=2740^\circ\text{K}$ (mp), it appears that a large fraction of the vacancy concentration in equilibrium at the melting point has disappeared. The vacancy concentrations calculated from the density difference would represent equilibrium temperatures of 1350° and 1500°C, respectively.

Harding⁵ reported the hydrostatic density of some high-precision niobium spheres as $8.5887 \pm 0.0011 \text{ g/cc}$ at 20°C, giving 8.5878 at 25°. Note that this is larger than the x-ray density reported here and higher than the x-ray density calculated by Harding. This disagreement could be due to tantalum impurities in his spheres. His density and the hydrostatic density reported here would agree if his samples contained 0.14 wt% Ta. His material was specified as "99.9±% pure."

I am grateful for the loan of the niobium sample from R. R. Soden and for the hydrostatic density measurements by Mrs. R. G. Baker. I am especially grateful to R. E. Jaeger for reviewing the manuscript.

¹ H. A. Bowman and R. M. Schoonover, J. Res. Natl. Bur. Std. 71C, 179 (1967).

² W. L. Bond, Acta Cryst. 13, 814 (1960).

³ R. L. Barns, Mater. Res. Bull. 2, 273 (1967).

⁴ C. S. Barrett and T. B. Massalski, *Structure of Metals*, (McGraw-Hill Book Company, New York, 1966), 3rd ed., p. 382.

⁵ J. T. Harding, J. Appl. Phys. 37, 928 (1966).

Correction to "Transition Probabilities for Some Ar II Laser States"

G. F. KOSTER

Department of Physics, Massachusetts Institute of Technology,
Cambridge, Massachusetts

AND

H. STATZ AND F. A. HARRIGAN

Raytheon Research Division, Waltham, Massachusetts

AND

C. L. TANG

School of Electrical Engineering, Cornell University, Ithaca, New York

(Received 15 March 1968)

In a previous paper¹ we have evaluated transition probabilities between certain states of ionized argon. Recently Professor N. Sobolev from the Lebedev Physical Institute pointed out to the authors that some calculations carried out in his institution agreed with our transition probabilities between laser states but disagreed by a factor of five from ours for transitions terminating in the ground state of ionized argon. Indeed our calculated transition probabilities from the lower laser states derived from the $3p^4s$ configuration to the $3p^5$ ground state should be five times larger than given in Ref. 1, Table V.

The oversight which occurred in our calculations is probably not readily apparent since we applied Eq. (10) of Ref. 1 consistently for transition probabilities between two excited states and for transitions between excited states and the ground states. The application of Eq. (10) of Ref. 1 was justified for transitions between excited states but not for transitions involving the ground state. Thus, the radiative lifetime of the lower laser states is affected.

It is probably of interest to show how the additional factor of five occurs. The error in Ref. 1 results from an oversight in the antisymmetrization of the wavefunctions with respect to the coordinates of the electrons. In Ref. 1 we obtained L - S coupled wavefunction components of the excited states by coupling a core wavefunction $\phi_m(1\cdots 4)$ made up of four $3p$ electrons to a running electron ($4p$ or $4s$) with wavefunction including spin $v_n(5)$. The subscripts m and n stand for the various quantum numbers of the core and running electron states. Obviously we obtain a wavefunction which has good quantum numbers of orbital angular momentum, spin angular momentum and total angular momentum by taking a linear combination of products $\sum_{mn} A_{mn} \phi_m(1\cdots 4) v_n(5)$, where the coefficients in essence are Clebsch-Gordan coefficients. All this was done correctly in Ref. (1) [Eqs. (8) and (9)]. In addition, the wavefunction has to be antisymmetrized with respect to the various electrons. Since the antisymmetrization process is identical for any combination of m and n in $\phi_m(1\cdots 4) v_n(5)$, we can show our point by restricting the analysis to just one term of the sum. We thus repress the indexes m and n and write for the wavefunction of a certain excited state symbolically

$$\psi_{e\pi\sigma} = (A/5^{1/2}) \phi(1\cdots 4) v(5). \quad (1)$$

In Eq. (1) we assume that ϕ is already antisymmetrized with respect to electrons 1 through 4. Thus the antisymmetrizer A can be taken to have the form

$$A = E - P_{15} - P_{25} - P_{35} - P_{45}, \quad (2)$$

where E is the identity and P_{15} , for example, is an operator that interchanges the space and spin coordinates of electrons 1 and 5.